Exceptional removal capacity of clenbuterol from aqueous solution by mechano-synthesized [Cu (INA)$_2$]-MOF via ball-mill

Marinah Mohd Ariffin[1], Usman Armaya'u[*1,2], Saw Hong Loh[1],
Wan Mohd Afiq Wan Mohd Khalik[1] and Hanis Mohd Yusoff[1]

[1]*Faculty of Science and Marine Environment, Universiti Malaysia Terengganu*
[2]*Faculty of Applied Sciences, Al-Qalam University Katsina, Nigeria*

Abstract. Copper-based Metal-organic framework (MOF) namely ([Cu (INA)$_2$]-MOF) is synthesized by ball milling and characterized using scanning electron microscopy (SEM) for the topography, microstructure, and elemental evidence determination, powdered X-ray diffraction (XRD) for the crystallinity measurement, thermogravimetric (TG) analysis was performed to determine the thermal stability of the material, and Fourier transformed infrared (FTIR) spectroscopy for functional groups identification. The use of [Cu (INA)$_2$]-MOF as hazardous removal material of β-agonists as persistent hazardous micro-pollutants in our environmental water is first reported in this study. The removal efficiency of the Cu-MOF is successfully determined to be 97.7% within 40 minutes, and the MOF has established an exceptional removal capacity of 835 mg L^{-1} with 95 % percent removal on Clenbuterol (CLB) even after the 5th consecutive cycle. The Langmuir model of the adsorption isotherms was shown to be more favourable, while the pseudo-second-order model was found to be favoured in the kinetics. The reaction was exothermic and spontaneous from a thermodynamic standpoint, and the higher temperatures were unfavourable for the adsorption study of the CLB. As a result, the studied MOF have shown promising properties as possible adsorbents for the removal of CLB in wastewater.

Keywords: ball-mill; *β*-agonists; clenbuterol; metal-organic frameworks (MOFs)

1. Introduction

The use of metal-organic frameworks (MOFs) has risen significantly in recent years, as porous coordination polymers with their high porosity and crystallization, controlled surface chemistry and functional groups, as well as specific electronic structure, among other properties, made its application easy and in higher demand for use in a variety of fields (Policicchio *et al*. 2017). In the chemistry of material sciences, MOFs are among the fastest-growing disciplines, not only because of their interesting structural topologies and their great diversities of pore sizes, but also because of their promise as functional materials in a wide range of applications (Dhaka *et al*. 2019). The fascination with MOFs derives from their unique properties, which distinguish them from other synthetic materials in that they have an ultra-high surface area, great crystallinity, homogeneity of pore diameters, and tunability of sizes. Their microporous structures have a surface area of 10000 m g^{-1} and high defined pore volumes of up to 2 cm^3 g^{-1}, allowing them to achieve high surface area and specific pore volumes. And were found to have open-framework structures, which allowed for the incorporation of guest species, such as solvents, during the synthesis procedure. A desolvation procedure might be used to eliminate these guest species, which could result in an empty framework

(Zango *et al*. 2020). So the framework's structural composition is dictated by the amount to which volatile solvents have been adequately removed or exchanged to allow either the formation of a really porous substance or the entrapment of other molecules inside the pore structure (Hu *et al*. 2019). The word porosity here refers to the presence of space in at least one crystal phase that may be filled by guest molecules, allowing for repeatable guest adsorption (Schneemann *et al*. 2014). For most applications, the pores of MOFs are often filled by solvent molecules, which must be removed in order to perform host–guest chemistry, such as catalysis, large pores are beneficial. As a result, mesoporous (openings between 20 and 500 Å) or even macroporous (openings more than 500 Å) materials are attractive. Having holes smaller than 20 Å in diameter results in strong interactions between gas molecules and the pore walls, which makes microporous materials excellent candidates for adsorption, storage, and separation applications in the chemical industry. When measuring these pore apertures, measurements are taken from atom to atom while removing van der Waals radii to yield the space accessible for guest molecule's entry (Kuppler *et al*. 2009).

The increased costs associated with conventional solvent-based synthesis of MOFs, as well as the environmental consequences of large-scale solvent usage, prompted researchers to seek for alternatives to solvent synthesis as a premium measure (Li *et al*. 2018). The oldest reported mechanochemical reaction may have been the grinding of cinnabar with acetic acid in a copper jar to produce elemental mercury in the 4th century BC (Soc *et al*.

---

*Corresponding author, Ph.D.,
 E-mail: p4222@pps.umt.edu.my

2012). Nowadays, people are paying greater attention to the uses of mechanosynthetic methods in the synthesis of materials that are both cost-effective and ecologically beneficial. It is becoming more popular for a variety of reasons, one of which being its ability to facilitate interactions between solids fast and quantitatively with either no additional of toxic and hazardous solvent or only minimum quantities.

Due to copper's abundance, low toxicity, and cheap cost, as well as the presence of a coordinatively unsaturated metal center in its structure and its pharmaceutical importance, the copper (II) metal organic framework ([Cu (INA)₂]-MOF) has turned into a significantly operational and cost-effective material (Mansano Willig *et al.* 2020). Also, for instance, some reports note the existence of structures constructed from rigid isonicotinate building blocks, like [Cu (INA)₂]-MOF (INA = isonicotinate) for the environmental clean-up of some toxic compounds like removal of a fluorescent dye (Tella *et al.* 2014), it has also been utilized for the catalytic activity (Truong *et al.* 2015) (Nguyen *et al.* 2017), as well as on adsorption of various metals (David and Dixon 2015), in extraction (Zhou *et al.* 2012), explorations of magnetic properties (Almáši *et al.* 2014), and the removal of polyaromatic hydrocarbons (PAHs) in water samples (Tella *et al.* 2016, Manousi and Zachariadis 2020).

On the other hand, the distribution, use, and manufacturing of medicines and related substances has resulted in the presence of organic pollutants in water, which has been a focus of government and researchers all over the world. Now a days the concern has shifted to identifying the various convenient methods of reducing and attempting to fix these impurities in our water as a result of widespread reports on the bad side-effects encountered in the environment (Armaya'u *et al.* 2022, Zango *et al.* 2020). This development arose after first Hignite's report on the occurrence of medicines in 1977-1978 (Hignite and Azarnoff 1977). Studies indicated that humans and animals excrete about 70% of the absorbed volume (of pharmaceuticals taken) as a combination of non-metabolized medicines and their conjugated metabolite (Sakai *et al.* 2016, Ternes 1998), these excreted drugs may wind up in sewage treatment facilities or in our environmental waterways, ultimately making their way into our drinking water. Despite these reports, an incredibly small number of pharmaceuticals of the more than three thousand medications listed being evaluated for their presence and environmental involvement in water, around 5% were analyzed for their trace presence and potential environmental impact (Salem *et al.* 2012). This presents a clear problem because our water habitats must have techniques for testing and removing trace pharmaceuticals as removing these polluting microenvironments from our water is of high importance (Yu and Wu 2011).

β-agonists are bronchodilator drugs that dilates the bronchi and bronchioles for airflow to the lungs, and are also used as a tocolytic treatment that inhibits uterine contractions to prevent premature labour (Slotkin and Seidler 2013). CLB is an aniline-like β-agonist 1-(4-amino-3,5-dichlorophenyl)-2-(tert-butylamino)ehanol (Salem *et al.*

Fig. 1 Model structure of Clenbuterol

2012) molecule with the chemical formula ($C_{12}H_{18}C_{l2}N_2O$) and structurally presented in Fig. 1 with a water solubility of 0.112 mg/mL and logP value of 2.33, having a molecular weight of 277 g/mol, and a pKa value of 9.29 (de Ridder *et al.* 2011). Generally, the molecular detail of CLB have a total of 35 bonds, containing 17 non-H bonds, 6 multiple bonds, 4 rotatable bonds, 6 aromatic bonds, 1 six-membered ring, 1 primary aromatic amine, 1 secondary aromatic amine, 1 hydroxyl group, and 1 secondary alcohol. As shown in the chemical structure of clenbuterol depicted in Fig. 1.

CLB is a predominant β-agonist drug used to treat asthma, a prevalent chronic respiratory condition with a complicated origin. Increased rates of neurodevelopmental problems, including autism spectrum disorders, have been related to its off-label usage for long-term treatment of preterm labor in pregnant women. It is typically administered via a variety of methods, the most common of which being inhalation, oral administration, and injection. In addition, β-agonists can be used in overdoses to treat certain respiratory diseases, which can result in serious side effects. Because higher doses of CLB and other β-agonists stimulate β-receptors, their presence at a certain level can pose a significant threat to human health, with symptoms including tachycardia, nervousness, muscle tremors, fatigue, confusion, headache, dizziness, chest distress, and heart palpitations (Sakai *et al.* 2016, Yan *et al.* 2016) to poisoning cases (Aboul-Enein and Serignese 1999). The possibility of long-term human health effects from β-agonist exposure through drinking water, as suggested by (Daughton and Ternes 1999), and their effects raised concerns about the continuous discharge of these compounds into the environment, as their presence has been confirmed in our domestic treated tap waters (Valcárcel *et al.* 2011, Rodil *et al.* 2012, Quintana *et al.* 2012, Petrović *et al.* 2014).

CLB is selected as the model analyte in this study owing to its negative environmental effects and toxicity to people and aquatic creatures because of its repeated introduction into the environment.

For quality assurance, quality control research of our wastewaters, as well as clinical and pharmaceutical research chemistry. The variety of wastewater treatment methods used for the removal and determination of β-agonists

includes non-pre-treatment approaches immunoassays (Liu *et al*. 2018) and sensors (Yang *et al*. 2019) as well as the chromatographic methods HPLC (Salem *et al*. 2012) and GC (Yu and Wu 2011) that need pre-treatment (pre-concentrations) of the samples before eventual analysis and determination were used. Whereas the removal techniques were focused on photo-degradation (Yan *et al*. 2017), oxidation (Lan *et al*. 2018), and adsorption (de Ridder *et al*. 2011, Selkälä *et al*. 2018). Because other techniques frequently produce intermediate and oxidation brands whose stability and toxicity are greater than the micropollutant even when they are successful in degrading them, adsorption was found to be the most favourable, simple, promising, inexpensive, and environmentally friendly method for environmental application. Additionally, because there is no accumulation of potentially toxic or carcinogenic substances, adsorption was found to be the most environmentally friendly method for environmental application. Therefore, researchers are working hard to find new types of adsorbents and novel ways of successfully removing contaminants. Adsorbents like molecularly imprinted polymers (MIP) (Tang *et al*. 2016), micro-grain activated carbon (μGAC) (Alves *et al*. 2018) as well as the anionic cellulose nanofibrils (Selkälä *et al*. 2018) were some of the limited adsorbents used for the adsorption of β-agonists in water.

The micro - porous and stable Cu-based MOF [Cu (INA)$_2$]-MOF is described here as an adsorbent for the new hazardous removal material of CLB in aqueous solution using a highly successful and ecologically acceptable (green) method of combining ball-mill mixing and heating of solid reactants. The present [Cu (INA)$_2$]-MOF is found to fulfil the MOF requirements among which that includes high thermal and chemical stability, acceptable porosity, avoiding large impurities and sustainability as suggested by (Stock and Biswas 2012).

2. Experimental section

2.1 Chemicals and materials

All the chemicals used in this project were of analytical standards, and they were utilized exactly as they were purchased. Sigma Aldrich (St. Louis, MO, USA) provided isonicotinic acid (98%), copper acetate monohydrate (Cu (CH$_3$COO)2H$_2$O) (98.5%), and clenbuterol sulfate for this study IT Tech Research Selangor, Malaysia, provided the sodium hydroxide (NaOH), methanol (99.5%), and hydrochloric acid (HCL).

2.2 Methodology

2.2.1 Synthesis of [Cu (INA)$_2$] MOF

The ball-milled synthesis was carried out using the (Tella *et al*. 2014) method with minor modifications. To summarize the synthesis method; copper acetate mono-hydrate (203 mg, 1 mmol) and isonicotinic acid (252 mg, 2 mmol) were carefully weighed in a stainless-steel ball mill vessel equipped with steel balls of 20 g, manufactured by

Retsch. The vessel was sealed, and milling was carried out for 10 minutes at room temperature at a speed of 25 Hz. The obtained product was then heated (desolvated) at 200 °C for 3 hours to remove the glacial acetic acid confined in the pores of the [Cu (INA)$_2$]-MOF, and the product was kept cool in a desiccator before being stored in the sample bottle and later used without any additional treatment during the experimental work.

2.2.2 Characterization

The synthesized [Cu (INA)$_2$]-MOF were subjected to several kinds of characterization. The Fourier transformed infrared (FTIR) was performed by (PerkinElmer FTIR spectrometer) to identify the functional groups, while the chemical identification of the adsorbent material was determined using the pH drift process of pHPZC, and the thermal stability (thermogravimetry) was determined using the Shimadzu TGA-50 Analyzer. Field emission scanning electron microscopy (FESEM) was used to determine topography, microstructure, and elemental evidence (EDX) using a Zeiss Supra 55 VP equipment, and powdered X-ray diffraction (XRD) was used to determine crystallinity using a Bruker D8 Advance X-ray Diffractometer (XRD).

2.3 Adsorption experiment

2.3.1 Preparation of Clenbuterol solutions

CLB (1000 mg L^{-1}) was produced as a stock solution in methanol by dissolving 100 mg in a 1000 mL volumetric flask. The produced solution was kept refrigerated at 4 °C (Selkälä *et al*. 2018) between the experiments. Daily, working solutions were prepared by diluting the appropriate quantity in the stock solution just before to use in the adsorption tests.

2.3.2 Batch adsorption experiment

A batch adsorption experiment was carried out at a varied concentration by diluting the stock solution with distilled water in steps of increasing concentration. The synthesized [Cu (INA)$_2$]- MOF were suspended in a conical flask (150 mL) containing 10 to 60 mg L^{-1} volumes of CLB at various starting concentrations with 1 mg g^{-1}, and the mixture was allowed to settle. The flask was then placed into a temperature-controlled incubator shaker (stacked shaker SKE 8000) and agitated at 150 rpm for 10 to 60 minutes. All experimental investigations were carried out at a temperature of 25 °C. At 10-minute intervals, about 2 mL aliquots of the sample solution were collected, and the filtrate solution was passed through a nylon syringe membrane (0.45 μm). The absorbance of the CLB in the filtered solution was measured at 262 nm (in triplicate in each) using a UV-Vis spectrophotometer (Shimadzu UV-1800) and quartz cuvettes. In order to calculate the percentage removal (% R), the amount adsorbed at a certain time interval (qt), and the quantity adsorbed at equilibrium (qe), the following equations were used: Eqs. (1)-(3) (Hong *et al*. 2019);

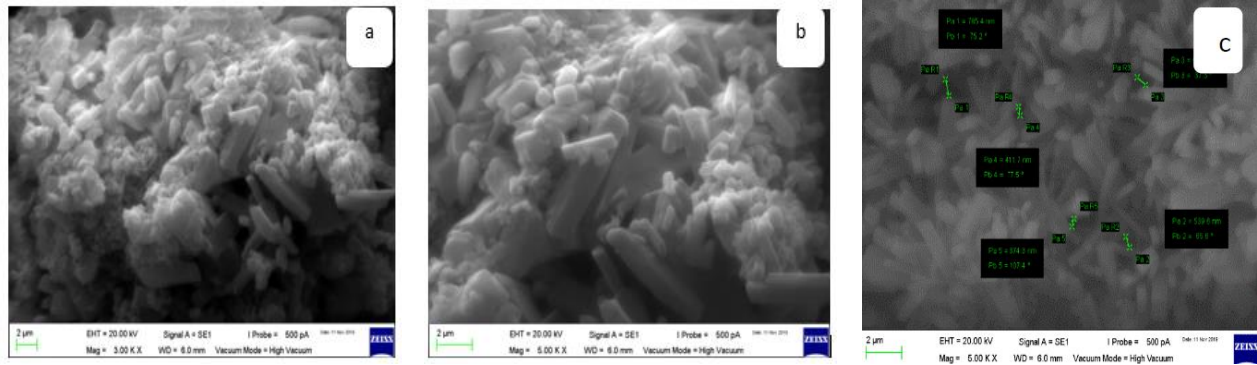$$\%R = \frac{(C_0 - C_e)}{C_0} X\ 100 \tag{1}$$

Fig. 2 SEM images of the [Cu (INA)$_2$]-MOF at a) 3.00 and b) 5.00 magnifications c) SEM image of [Cu (INA)$_2$]-MOF material showing a various pore aperture/area with a high value of Pa 785.4 nm at 5.00 magnifications

$$q_t = \frac{(C_0 - C_t)V}{W} \quad (2)$$

$$q_e = \frac{(C_0 - C_e)V}{W} \quad (3)$$

For CLB, Co (mg L^{-1}) represents the starting concentration, Ct (mg L^{-1}) represents the concentration at a time (minutes), and Ce (mg L^{-1}) represents the equilibrium concentration. Adsorbent's dry weight (grams) and solution volume (L).

Also, effects of pH were examined by varying the solution pH between 3, 5, 7, 9, 11, and 13 by adding 0.1N NaOH or 0.1N HCL and making up to 30 mg L^{-1}, and effects of temperature were investigated by varying the temperature between 25, 30, 35, 40, 45, and 50 °C. 1 mg g^{-1} adsorbent dose was used in all the concentrations of CLB ranging from 10, 20, 30, 40, 50 and 60 mg L^{-1}.

2.4 Regeneration study

The regeneration and reusability of the adsorbent were also evaluated, as we observed that some of the previous studied does not carry out this study. Following the decanting of the supernatant (filtrate), [Cu (INA)$_2$]- MOF (adsorbent) residue was washed with 50 mL absolute methanol and then rinsed with distilled water 5 times, after which the washed [Cu (INA)$_2$]- MOF was vacuum dried for 3 h at 100 °C and stored in the desiccator until reuse. The regenerated [Cu (INA)$_2$]- MOF was employed as the adsorbent in a 5-cycle adsorption experiment under the same optimal conditions as the batch adsorption experiments performed earlier.

2.5 Thermodynamics

The analysis of thermodynamics, which is based on temperature differences, offers information on the nature and characteristics of the adsorption process. The temperature dependence of the adsorption process was used to derive the thermodynamic parameters of the process, such as Gibbs free energy change (ΔG°), standard enthalpy change (ΔH°), and entropy change (ΔS°), using Eqs. (4)-(6) as obtained from Van't Haff (Saruchi and Kumar 2019).

$$\Delta G° = - \; RT\ln K_d \quad (4)$$

$$K_d = \frac{q_e}{c_e} \quad (5)$$

$$\Delta G° = \Delta H° - \; T\Delta S \quad (6)$$

The Gibbs free energy change is represented by the constant ΔG° (kJ mol^{-1}). In these equations, R denotes the universal gas constant (J K mol^{-1}), and T is the temperature, K often referred to as the distribution coefficient, qe (mg g^{-1}) this numerical value corresponds to the proportion of CLB adsorbed on MOF surfaces to the concentration of adsorbates (Ce, mg L^{-1}) while the system is in steady state. The ΔH° (kJ mol^{-1}) and ΔS° (Jmol^{-1}K) variables, which reflect the process's enthalpy and entropy changes, respectively. The values of the parameters were derived using plots of InKc versus 1/T derived from the data.

3. Result and discussion

3.1 Characterization of [Cu (INA)$_2$]-MOF

The characterized [Cu (INA)$_2$]- MOF was shown to be successful as the SEM provides detailed resolution images of the sample by displaying a focussed electron beam across the surface and detecting secondary or backscattered electron signal. The SEM image of [Cu (INA)$_2$]- MOF material are presented in Figs. 2(a) and (b) under different magnifications resembles the images reported by Tella (Tella *et al*. 2014), while in Fig. 2(c) a various pore aperture/area with a high value of Pa 785.4 nm at 5.00 magnifications is represented. While FESEM images are presented in Fig. 3(a) and (b) with 3.7 mm and 3.5 mm magnifications respectively. The morphology of the MOF from the FESEM results resembles a rectangular bar shape with a rough surface that makes the porous nature of the mechanically synthesized [Cu (INA)$_2$]-MOF possible. The images indicated higher magnifications with clearer [Cu (INA)$_2$]- MOF crystal details. And the EDX results of both the SEM and FESEM presented in Fig. 4(a) and (b) respectively showed the present of copper, carbon, nitrogen, and oxygen as expected elements present in the material.
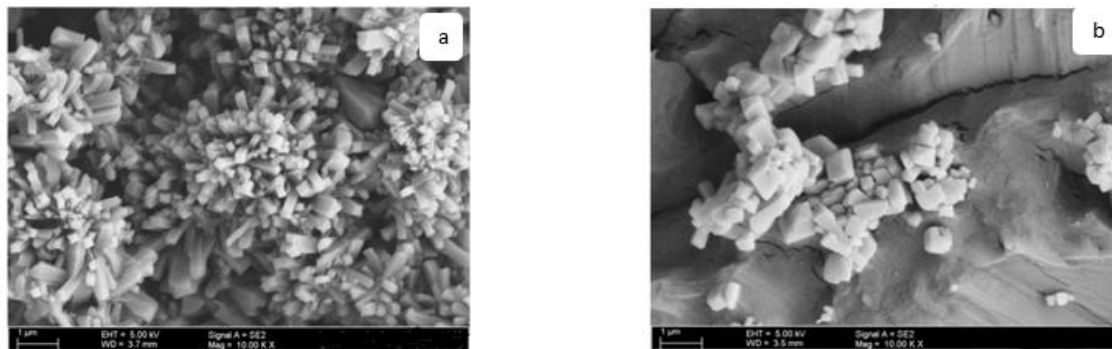
Fig. 3 FESEM images of the [Cu (INA)$_2$]-MOF at (a) 3.7 mm and (b) 3.5 mm both at 10.00 magnifications respectively
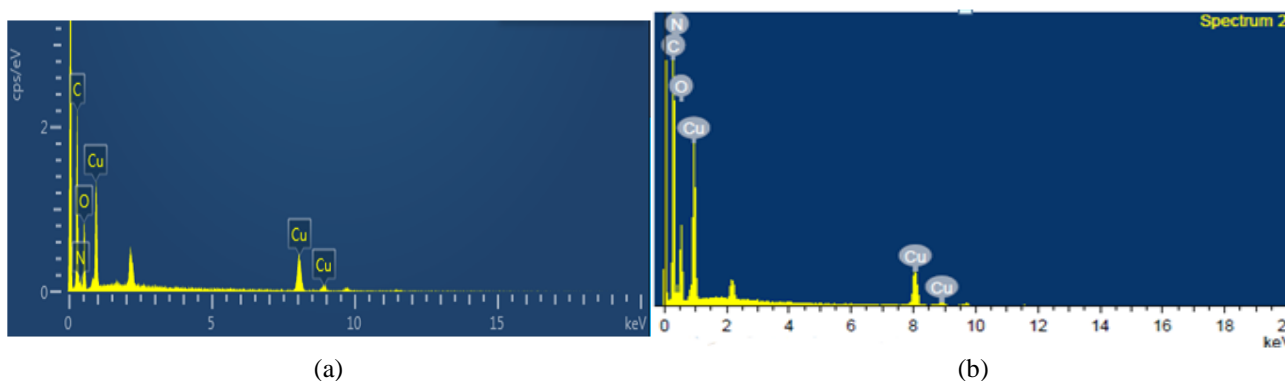

(a)   (b)

Fig. 4 EDX Spectrums (a) SEM and (b) FESEM of the [Cu (INA)$_2$]-MOF indicating the elemental composition in the materials
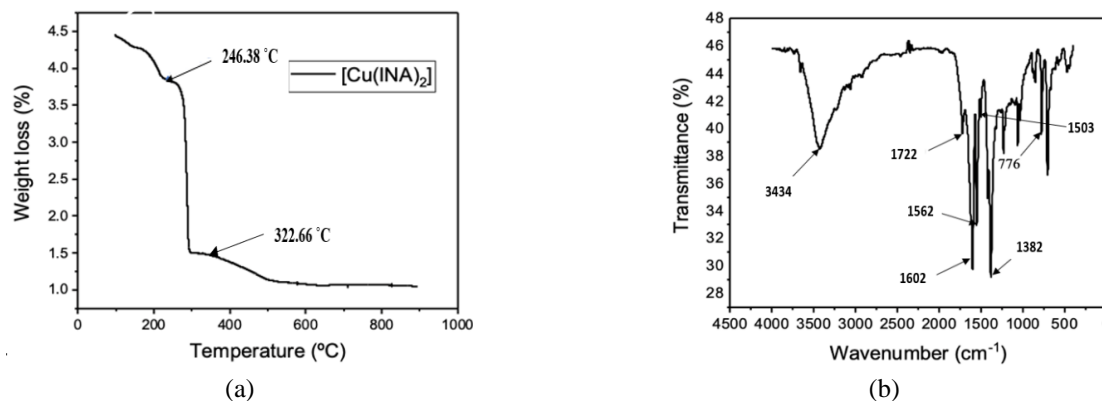

(a)   (b)

Fig. 5 (a) Thermogravimetric analysis (TGA) (b) FTIR spectrums of the [Cu (INA)$_2$]-MOF

The thermogravimetric analysis (TGA) was done with a starting mass of 4.642 mg (shown in Fig. 5a below), and the heating rate was kept constant from 100.00 °C to 900.00 °C at 10.00 °C/min for the whole TG analysis. The thermograms showed that the [Cu (INA)$_2$]-MOF material was stable up to 250 °C, which removed the solvent molecules in the framework. The whole analysis showed two major weight losses between 246.38 °C and 322.66 °C, between 82.292 % and 32.165 %, which were caused by the continued loss of guest water molecules and acetic acid (Liu *et al*. 2001).

Fig. 5(b) depicts the [Cu (INA)$_2$]-MOF's infrared spectra in the visible range (FT-IR). - OH extending from the copper acetate and isonicotinic acid linker, which served as the secondary building components of the MOF, was responsible for the significant peak at 3434 cm^{-1}. The presence of a strong signal at 1602 cm^{-1} in the spectra suggested that the isonicotinic acid linker had been deprotonated, which was confirmed by the results (Nakamoto 2006). The formation of the peak at 1562 cm^{-1} was due to υCOO– asymmetric stretching, whereas the appearance of the peak at 1503 cm^{-1} was due to υCOO– symmetric stretching owing to the organic linker. The stretching vibration at 1722 cm^{-1} demonstrates that the isonicotinic acid is completely coordinated (Tella *et al*. 2014). In addition, the formation of the Cu-O coordination
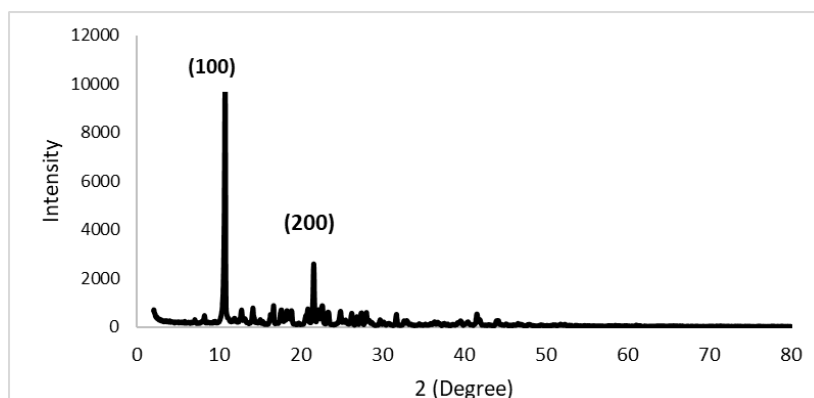
Fig. 6 XRD patterns for the Cu [(INA)2]-MOF with the value of the Miller indices (hkl), which define the reciprocal axial intercepts of a plane of atoms with the unit cell; more specifically, the (hkl) plane of atoms intercepts the unit cell
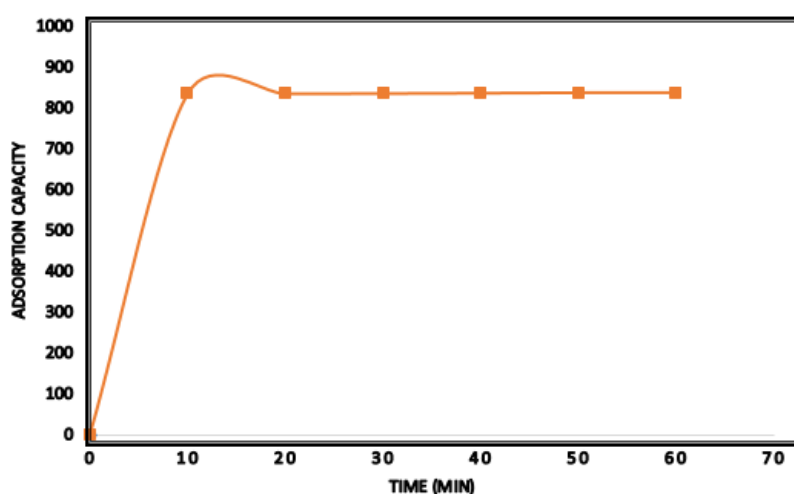

Fig. 7 Effect of contact time for adsorption of CLB onto [Cu (INA)$_2$]-MOF

bond is shown by the absorption band at around 776 cm^{-1} (Nakamoto 2006). The signal at 1382 cm^{-1} demonstrates the stretching of the C=N bond due to the contribution of nitrogen from the pyridine ring to the coordination sphere (Tella *et al*. 2014, Toma *et al*. 2006).

The results of the XRD patterns are presented in Fig 6. When compared with that of the X-ray diffraction pattern of the simulated/calculated pattern obtained from Cambridge Structural database for [Cu(INA)$_2$]-MOF Cambridge Crystallographic Database (CCD) code UFUMUD and the material prepared in a literatures reported and published by Pichon *et al*. (2006), and Lu and Babb (2002) the results showed that the synthesized compounds closely matched the compound synthesized via Mechanosynthesis procedure in our lab.

3.2 Removal studies

3.2.1 Effect of contact time and concentration

Adsorption experiments involving CLB, and adsorbent systems need the optimization of contact time duration in order to achieve a suitable equilibrium between the two systems. In this study, the removal of CLB was studied at different concentrations (10–60 mg/L), with contact times

ranging from 10–60 minutes, under optimum pH, adsorbent dose, and temperature conditions pH 11, 0.01 g/L, and 25 °C respectively. As shown in Fig 7, the impact of contact time on the removal of CLB was investigated. The results revealed that the CLB was removed effectively, with equilibrium being reached in a shorter time because of favorable interactions between the pollutants and the MOF. The removal of CLB was shown to happened because; there is a high availability of adsorption sites in the early stage, but as time progresses, the availability and number of available sites declines (Saruchi and Kumar, 2019). This result was consistent with the findings of many adsorption experiments that had been previously performed (Isiyaka *et al*. 2020, Zango *et al*. 2020).

3.2.2 Effects of pH on clenbuterol removal

The pH of the solution is one of the most influential parameters on the adsorption behaviour of any adsorbent material (Kyzas *et al*. 2015, Benhafsa *et al*. 2022). The impact of pH on the adsorption of CLB onto the [Cu (INA)$_2$]-MOF was investigated at pH values ranging from pH 3, pH 5, pH 7, pH 9, pH 11, and pH 13 in our laboratory. As shown in Fig. 8(b) an increase in the % removal of the analyte in accordance with an increase in pH value was
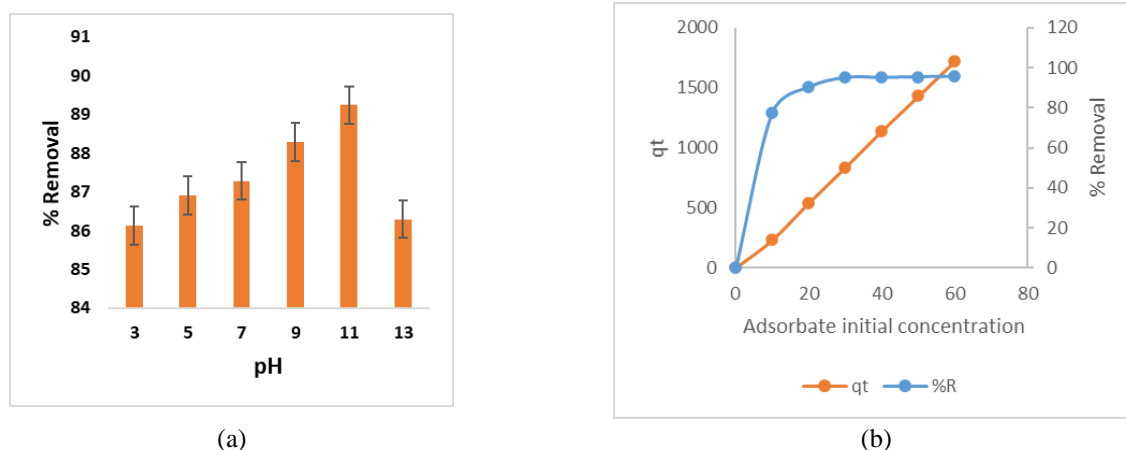
Fig. 8 (a) Effect of pH on the adsorption of Clenbuterol onto [Cu (INA)$_2$]-MOF (b) Correlated effects of adsorbate initial concentration of the percent removal and the adsorption capacity

observed, indicating a strong effect of the pH of the solution on the efficacy of [Cu (INA)$_2$]-MOF for CLB's adsorption. A neutral pH value (pH 7) was shown to be accompanied by the start of good adsorption results which increase with the increase in the pH of the solution. With a pk$_a$ of 9.72, CLB's species are generally positively charged in solution at pHs ranging from 3 to 10. This is due to the fact that CLB is a secondary amine as well as an aniline-type agonist in which pH ranges of 11-12 are reportedly ideal for their extraction and adsorption (Spisso *et al*. 2000). Increasing the pH value of the solution resulted in an increase in adsorption efficiency, which reached more than 89 % at pH 11, as well as a very high adsorption capacity of more than 835.9 mg g^{-1}, indicating that the CLB adsorption process on Cu-MOF is favored because of this phenomenon.

3.2.3 Effects of adsorbate initial concentrations on [Cu (INA)$_2$]-MOF dosage

Adsorbent material that is considered excellent and worthy of being used must be capable of achieving maximal adsorption of adsorbate removal at the lowest attainable dose in the shortest amount of time (Zango, Abu Bakar, *et al*. 2020). The influence of the MOF dosage on CLB elimination was investigated across a range of 10 mg L^{-1} to 60 mg L^{-1} of CLB concentrations using the lowest possible dosage of 1 mg g^{-1}. In this study, it was found that the increase of the concentration of CLB corresponds with the increase in the percentage removal as well as the increase in adsorption capacity up to the equilibrium stages around 30 mg L^{-1} bringing the % removal around 95 % and 835 mg g^{-1} adsorption capacity at equilibrium (Fig 8b). A greater mass of MOF would only adsorb a limited amount of CLB owing to the reduction in surface area of contact between MOF and adsorbate as the surface area of contact between the two increases. A research by Ariyee (Aryee *et al*. 2021) conducted recently described a situation similar to this study.

3.3 Analyses of surface chemistry and statistical models

Kinetic models were developed to predict the most likely processes of adsorption as well as the rates at which they occurred. It gave the most important variables that influence the affinity of the adsorbent to the adsorbate, which is the primary goal of the adsorption process. The adsorption capacity, mass transfer, diffusion control, and chemical reaction are some of the variables that influence the controlled adsorption process mechanism. The kinetic parameters provided information for modelling and designing adsorption processes, and the data generated is subjected to most prominent models, namely; pseudo-first-order, pseudo-second-order, and intra-particle kinetic models and the model that fits best is regarded as the best to describe the process as they are used in the present study. While Longmuir, Freundlich, and Temkin isotherm models were used to explain the relationship between the quantity of adsorbate adsorbed and the concentration of dissolved adsorbate in the liquid at equilibrium. The experimental isotherm and developed isotherm models were typically defined using several equations, whereas equilibrium isotherms are utilized to determine the capacity of synthesized [Cu (INA)$_2$]-MOF. The interaction between the [Cu (INA)$_2$]-MOF and the CLB was explained using these isotherm models. Furthermore, all these models were fitted with statistical regression analysis to define the coefficient of determination (R^2), adjusted coefficient of determination (adj R^2), root means square error (RMSE), and Akaike information criterion (AIC) as criteria for evaluating the best-fitted model performance using the eqs 7- 9 below respectively as presented from (Dotto *et al*. 2013, Zango *et al*. 2020) research.

3.3.1 Kinetic study

A full clarification of the mechanism and the rate-controlling step that defines the efficiency of adsorption is obtained from this model study.

3.3.2 The pseudo-first-order kinetic model

$$q_t = q_e (1 - exp (-K_1 t)) \quad (7)$$

The values q_e and q_t (mg/L) are the amount of the CLB adsorbed at a certain time t (min^{-1}) and at equilibrium respectively, while the pseudo-first order rate constant is

Table 1 Adsorption kinetics parameters for the removal of Clenbuterol on to the [Cu (INA)$_2$]-MOF

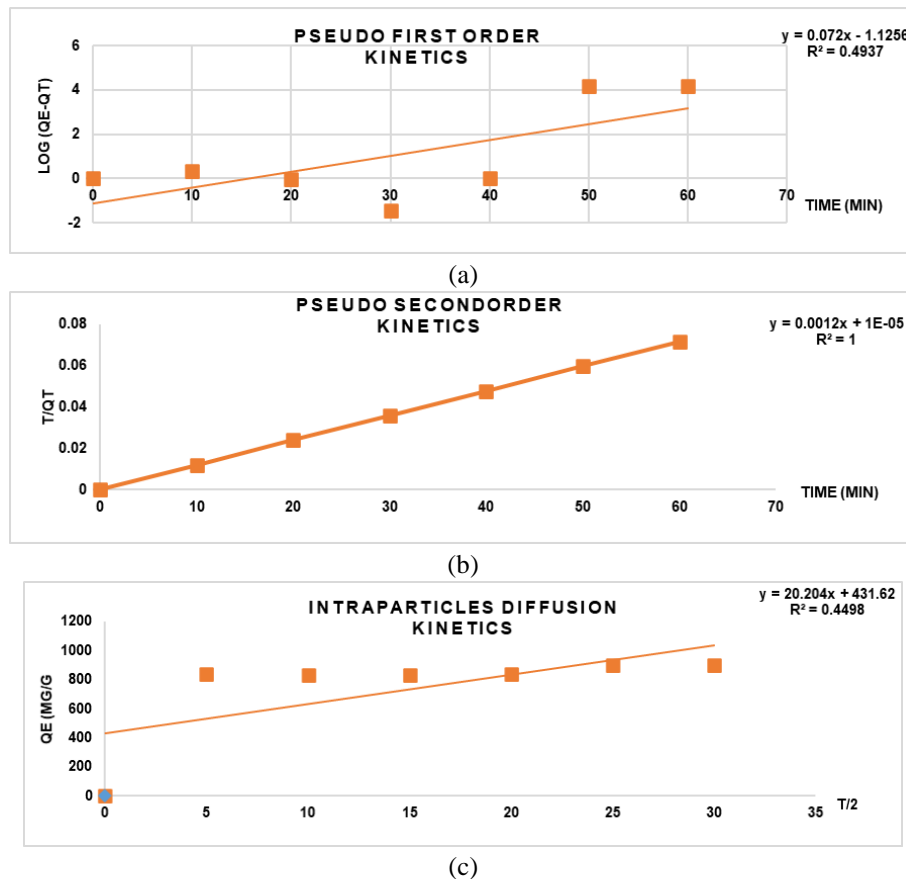| Pseudo-first order	(mg g^{-1})	$q_{e, exp}$ (mg L^{-1})	$q_{e, cal}$ (mg L^{-1})	K_1 (min)$^{-1}$	R^2	R^2adj	RMSE	AIC
	1	835.95	3.0821	0.072	0.4937	0.542	14.038	27.864
Pseudo-second order	(mg g^{-1})	$q_{e, exp}$ (mg L^{-1})	$q_{e\,cal}$ (g mg^{-1})	K_2 (g mg^{-1} min^{-1})	R^2	R^2adj	RMSE	AIC
	1	835.95	833.33	144	1	1	0.016	-48.38
Intraparticle diffusion	(mg g^{-1})		K_p (mg^{-1} g^{-1} min$^{1/2}$) C		R^2	R^2adj	RMSE	AIC
	1		20.204	431.62	0.4498	0.607	5.863	22.790

(a)

(b)

(c)

Fig. 9 (a) Pseudo first order kinetics of the adsorption study of Clenbuterol EDX Spectrums (b) Pseudo second order kinetics of the adsorption study of CLB (c) Intraparticle diffusion kinetics of the adsorption study of CLB

represented as K_1 (mg/L/min) in the equation obtained from (Saruchi and Kumar 2019, Zango *et al*. 2020).

3.3.3 The pseudo-second-order kinetic model

The availability of adsorption sites, also regarded as the process driving factor, provides the basis for this kinetic model. It may also be used to determine the rate of adsorption, expressed mathematically as;

$$q_t = \frac{t}{\left(1/_{k_2 q_2{}^2}\right) + \left(^t/_{q_2}\right)} \qquad (8)$$

q_2 is the theoretical value of the adsorption capacity (mg/L/min) and K_2 is the rate constant of the pseudo-second-order model.

3.3.4 The intra-particles diffusion kinetic model

This model is used to figure out how the adsorbate molecules penetrate the adsorbents and how the rate controlling phase in the adsorption process works. It is expressed mathematically as

$$q_t = k_p\, t^{1/2} + C \qquad (9)$$

where k_p is the intraparticle diffusion rate constant (mg/L/min) (Perrotti *et al*. 2019)

While the equations for the statistical regression analysis namely R^2, adj R^2, RMSE, and AIC as criteria for evaluating the best-fitted model performance are given as in Eqs. (10)-(13).

$$R^2 = 1\frac{\Sigma\left(q_{e\,exp} - \overline{q}_{e\,model}\right)^2 - \Sigma(q_{e\,exp} - q_{e\,model})^2}{\Sigma(q_{e\,exp} - \overline{q}^-_{e\,exp})^2} \qquad (10)$$

$$RMSE = \sqrt{\sum_{n=1}^{i} (q_{e\ exp} - q_{e\ model})^2} \qquad (11)$$

$$AIC = n ln\left(\frac{SSE}{n}\right) + 2n_p + \frac{2n_p(n_p + 1)}{n(n_p + 1)} \qquad (12)$$

The general terms $q_{e\ exp}$ and $q_{e\ model}$ denote experimental and model/calculate model adsorption capacities, respectively, with $\bar{q}$ is the average of q experimentally measured values, n is the number of observations, SSE is the sum of squared errors obtained, and p is the number of parameters.

The values of the parameters involved are shown in Table 1 while Figs. 9(a)-(c) show the graphical representations of the three studied models respectively. Among the models tested, pseudo-second order was shown to better explain the adsorption data in terms of greater R^2, as well as lower RMSE and AIC values, than the compared other models. Moreover, the estimated qe (mg g^{-1}) values are more consistent with the experimental findings in the pseudo-second order model.

3.3.5 Langmuir Isotherm

It is assumed in this model that the adsorbent has a limited number of identical sites and that the effects of monolayer adsorption are considered. It therefore describes adsorptions onto homogeneous adsorbent surfaces when the adsorbate molecules interact with the adsorbent surfaces. The mathematical representation of the model is given in Eqs. (13) and (14):

$$\frac{C_e}{q_e} = \frac{1}{K_L q_m} + \frac{1}{q_m} C_e \qquad (13)$$

$$R_L = \frac{1}{1 + C_0 K_L} \qquad (14)$$

where q_m and K_L represent constants that describe the adsorption capacity and adsorption energy, respectively, and R_L is a dimensionless parameter that represents the process' favorability in adsorption. R_L >1, negative (Unfavorable); $0 < R_L < 1$, positive (Favorable); and, if, $R_L = 1$, linear.

3.3.6 Freundlich Isotherm

With this model, the non-identical adsorbents with heterogeneous surfaces can be explained. The model is stated in the following way presented in Eq. (15):

$$q_e = K_F C_e \; 1/n \qquad (15)$$

K_F in (mg/g) represent the Freundlich Isotherm constant which signifies the adsorption capacity, while the value $1/n$ represent the adsorption intensity which is represented as the slope.

3.3.7 Temkin Isotherm

This model considers the indirect interaction between adsorbate molecules and the adsorbent and explains how the heat of adsorption reduces as the amount of adsorbate molecules covered decreases. It is provided by Eq. (16)

Table 2 Isotherm parameters for adsorption of Clenbuterol onto [Cu (INA)$_2$]-MOF

Isotherm Model	Parameter	Cu(INA)$_2$ Clenbuterol
Langmuir	q$_m$ (mg L^{-1})	833.3
	K$_L$ (L mg^{-1})	6024
	R$_L$	55 x 10^{-6}
	R^2	0.9918
	R^{2}adj	0.114
	RMSE	0.018
	AIC	-46.452
Freundlich	K$_F$ (mg g^{-1})	1.5959
	N	0.00165
	R^2	0.1258
	R^{2}adj	0.093
	RMSE	0.020
	AIC	-45.193
Temkin	A (mg g^{-1})	1.00114
	b$_T$ (kJmol^{-1})	1110.4
	R^2	0.9887
	R^{2}adj	-0.095
	RMSE	34.743
	AIC	44.143

below

$$q_e = \frac{RT}{b_T} \ln k_T\, C_e \qquad (16)$$

where bT and kT is the Temkin heat of adsorption (KJ mol^{-1}) and equilibrium binding constant corresponding to the optimum binding energy (L g^{-1}), respectively. Whereas T is an absolute temperature and R is the Universal gas constant 8.314 (mol^{-1} K^{-1}), respectively. The parameter was determined by plotting the linear functions of lnqe against lnCe.

The results obtained for the R^2, RMSE, and AIC were more satisfactory to the Langmuir model than the values of the other models as shown in Table 2 and the graphical representations in Fig 10 (a) - (c). The RL values obtained were smaller than unity, which means the process was favorable and that the [Cu (INA)$_2$]-MOF formed monolayer contacts with the CLB molecules. Therefore, the Cu-based MOF used had homogeneous adsorption sites that resulted in greater adsorption of CLB.

3.4 Thermodynamics of the adsorption study

Thermodynamics studies were carried out to determine the impact of temperature variations by taking different ranges of temperatures from 298 K, 303 K, 308 K, 313 K, 318 K, and 388 K on the adsorption process under the same conditions as those used in batch adsorption experiments. According to the Van't Hoff equations, the parameters ΔG°, ΔH°, and ΔS°changes were deduced from the values of the parameters.
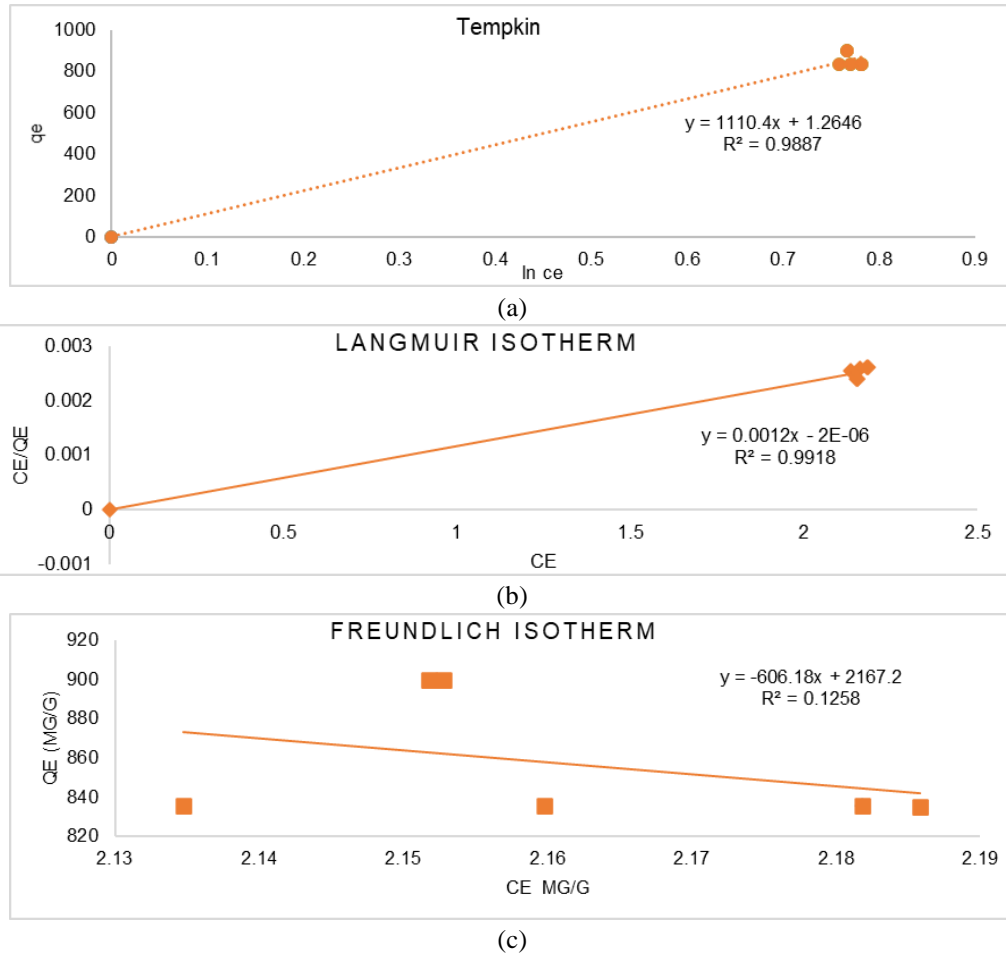
Fig. 10 (a) Temkin Isotherms model of the adsorption study of CLB (b) Langmuir Isotherms model of the adsorption study of CLB (c) Freundlich Isotherms model of the adsorption study of CLB
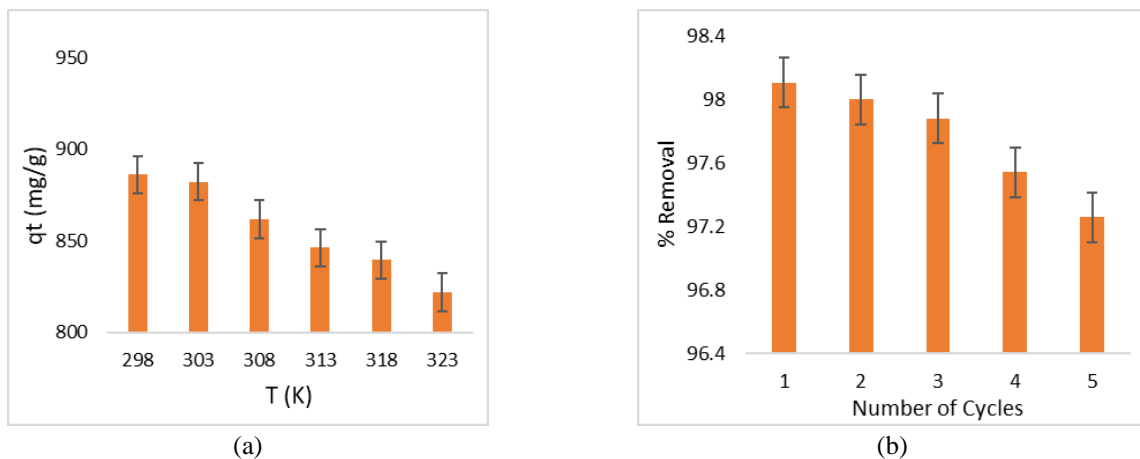

Fig. 11 (a) Effect of temperature on the adsorption of Clenbuterol on [Cu (INA)$_2$]-MOF (b) Reusability and regeneration ability of the [Cu (INA)$_2$]-MOF for the adsorption of Clenbuterol

From the results of the thermodynamics experiment (Fig 11a and Table 3), the adsorption capacity values of the MOF dropped from 886 mg g^{-1} (as temperatures rise) to around 822 mg g^{-1}. The adsorption was proven to be SPONTANEOUS based on the negative values of ΔG° obtained as the temperature raised the reaction occurred without any energy input. The positive values of enthalpy change ((ΔH°) indicated the products of the reaction gained energy, making it ENDOTHERMIC, while the positive value of entropy change as the degree of randomness ΔS°at the solid/liquid interface as well as structural changes in the adsorbent and adsorbate, and the process of adsorption is validated as CHEMISORPTION and RANDOM It also reveals the adsorbent's affinity for the adsorbate.

Table 3 Thermodynamic parameters for the adsorption of CLB onto [Cu (INA)$_2$]-MOF

Temp (K)	$\Delta G°$ (kJ/mol)	$\Delta H°$ (kJ/mol)	$\Delta S°$ (J/mol/K)
298	-0.01307		
303	-0.01329		
308	-0.01352	0.0707	0.0441
313	-0.01373		
318	-0.01395		
323	-0.01417		

Table 4 Adsorbents reported for the removal of CLB from water

Adsorbent material	Equilibrium time	Q $_{max}$ (mg/g)	Percentage Removal	Analytes	Reference
MIP@CIP	20 min	7.34	74.08-99.17 %	Clenbuterol	(Tang *et al.* 2016)
Ui-66 MOF	60 min	160	80 %	Clenbuterol	(Yang *et al.* 2019)
MIP@UCPs prove	20 min	2.18	81.66-102.46 %	Clenbuterol	(Tang *et al.* 2015)
Al (III)-MOF (BUT-19)	30 min	294.1	84 %	Clenbuterol	(Lv *et al.* 2021)
[Cu (INA)$_2$]-MOF	40 min	835	95 %	Clenbuterol	Present study

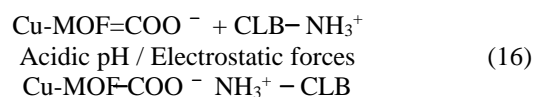## 3.5 Regeneration, usability and comparison studies

The ease with which the MOF were able to recover following active batch adsorption experiments demonstrated their potential as an adsorbent for the removal of CLB from solution as shown in Fig. 11(b), even after the fifth use, the percentage removal achieved in all the cycles were very efficient with more than 97 % removal efficiency, indicating the adsorbent's reusability.

A comparison study with other available earlier reported adsorbent material was presented in Table 4 to ascertain the efficiency of the presently studied adsorbent material.
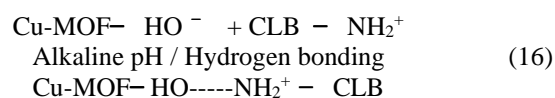
3.6 Expected Mechanisms for the adsorption

Furthermore, the surface properties of the [Cu (INA)$_2$]-MOF material, such as surface charge and the protonation-deprotonation shift of functional groups (such as carboxylic (–COOH), hydroxyl (–OH), and amine (–N–) on the active sites of the MOFs' surface were significantly affected as the pH varied over the range of pH 3 to pH 11, which could significantly change the adsorption of organic pollutants. It is evident that the chemical characteristics of the substance (CLB) and the MOF layers, under various pH circumstances, play an important role in the adsorption process. CLB is a secondary amine that has an acidity constant (pKa) more than 9.0, therefore, CLB specie is found in solution largely in positively charged form when the pH is adjusted to an operational level (pH 3–9). In addition, the [Cu (INA)$_2$]-MOF has a positively charged state for the particles in the pH values above pH 4 evaluated; however, the number of negatively charged sites on the Cu-MOF dropped as the pH of the system increased. Thus, at strong basic conditions is where the highest removal was observed, despite the fact that the magnitude of the negative charge on the Cu-MOFs surface is decreased compared to alkaline conditions, electrostatic forces between the negatively charged groups of Cu-MOFs (i.e., –COO) and the positively

ones of CLB (mainly the protonated amino groups –NH^{3+}) shown in Eq. (17) still exist and may play dominant roles in the drugs adsorption.

$$Cu\text{-}MOF\text{=}COO^- + CLB\text{−}NH_3^+$$
$$\text{Acidic pH / Electrostatic forces} \quad (16)$$
$$Cu\text{-}MOF\text{−}COO^-\ NH_3^+ - CLB$$

The CLB's adsorption onto the MOF material was presumably also governed by the oxygen-containing contents of the [Cu (INA)$_2$]-MOF and the structure of the compounds when they were exposed to alkaline circumstances (pH 8, 9, 10). Under these conditions, an increase was shown in the number of negative charges on the adsorptive sites of the surface of the [Cu (INA)$_2$]-MOF, whereas an increase was seen in the positively charged manner of the clenbuterol. Despite this, the removal of CLB is still affected by the electrostatic attraction that exists between the positively charged groups of clenbuterol and the negatively charged groups of [Cu (INA)$_2$]-MOF (mostly the protonated amino groups of CLB). Additionally, surface-bridging of organic molecules through H-bonding is highly facilitated due to the presences of -OH functional groups, (Eq. 18) which suggests that adsorption mechanisms are also affected by hydrogen bonds between a) the hydrogen atoms of hydroxyl groups of [Cu (INA)$_2$]-MOF and some nitrogen atoms of amino groups of the CLB molecules; b) the oxygen atoms of hydroxyl groups of [Cu (INA)$_2$]-MOF and hydrogen atoms of amino groups of CLB (Kyzas *et al.* 2015).

$$Cu\text{-}MOF\text{−}HO^- + CLB - NH_2^+$$
$$\text{Alkaline pH / Hydrogen bonding} \quad (16)$$
$$Cu\text{-}MOF\text{−}HO\text{-----}NH_2^+ - CLB$$

The structural characteristics of CLB may be connected to the greater removal found for it (Fig. 1). CLB has a phenylaminoethanol group, which gives it an aromatic structure it's molecular form can interact with other
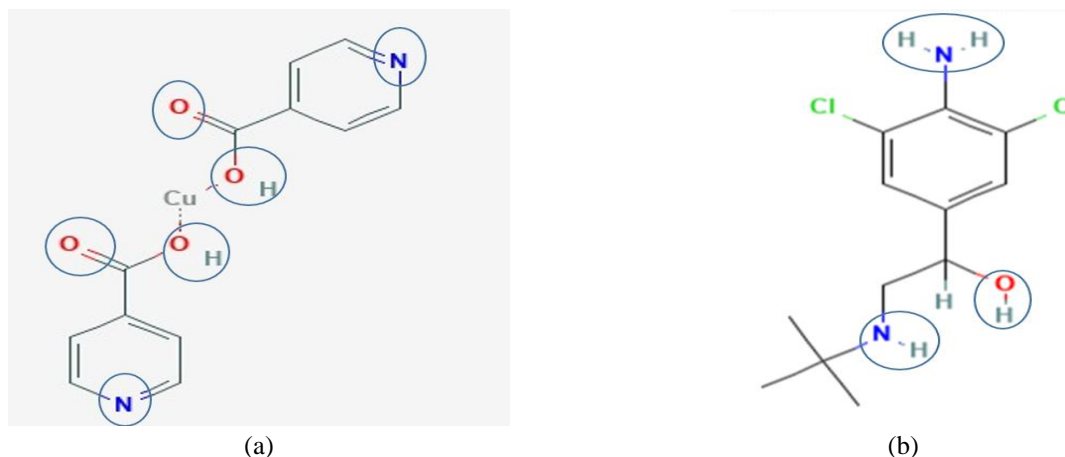
(a)   (b)

Fig. 12 (a) and (b) the structures of [Cu (INA)$_2$]-MOF and the Clenbuterol Model demonstrating the possible adsorptive interactive sites respectively

molecules and with itself through hydrogen bonds. It can act as a hydrogen donor by way of its secondary amine and hydroxyl groups, and it can also act as a hydrogen acceptor by way of its oxygen and secondary amine groups, as well as through a hydrogen bond with its extra amide group. This suggests that the hydrophobic effect does not predominate in the adsorption of CLB onto [Cu (INA)$_2$]-MOF material, rather direct interactions with functional groups on [Cu (INA)$_2$]-MOF through H-bonding would play important roles in CLB adsorption. These results can be viewed in conjunction with those of Mr. Yoon (Song and Jhung 2017) and Hussain (Hasan and Jhung 2015), that have examined various mechanisms to explain how liquids, such as water and fuel, can be adsorbed to MOF, including electrostatic interactions, coordination, π-complexation, H-bonding, and acid-base interactions. The structures of [Cu (INA)$_2$]-MOF and the CLB Models showing the possible adsorptive interactive sites is presented in Figs. 12(a) and (b) respectively.

4. Conclusions

The mechanochemical synthesis of [Cu (INA)$_2$]-MOF was carried out employing ball-milling machine, and the product was characterized using a variety of characterisation methods. The presence of active functional groups in the [Cu (INA)$_2$]-MOF was shown by the FTIR examination of the material, while the TG study revealed the disintegration of the framework at 534.32 °C, with good thermal stability of the framework. Aspects of the [Cu (INA)$_2$]-MOF's crystallinity were also shown by the XRD spectra, with the strongest peaks occurring at 2θ 10.76 and 22.5 °C, which corresponded to the main peaks previously described in the literatures and a hkl of 100 and 200 on the corresponding peaks. Results from this research show that [Cu (INA)$_2$]-MOF can efficiently remove CLB from water at concentrations as low as 1 mg g^{-1}, with a maximum adsorption capacity of 882 mg g^{-1} and an excellent removal efficiency of 95 % after just 40 minutes under an alkaline pH of 11 and an increase in adsorbate concentration from 10 mg L^{-1} to 60 mg L^{-1} resulted in a increased percentage of adsorbed material. The statistical fits of R^2, Adjusted R^2, RMSE, and AIC, was shown to be more favorable to pseudo-second-order model based on the kinetics of the process. While good Langmuir model fit the statistical isotherm of the process. The thermodynamics study revealed an endothermic process, with adsorption effectiveness decreasing as temperature was rose. The reusability study revealed the MOFs' adsorption efficiency of up to 5 cycles. This research study has shown that [Cu (INA)$_2$]-MOF forms a monolayer contact with CLB and forming an outstanding homogeneous adsorption of CLB from environmental water, and therefore recommended for its application in water remediations and removal of CLB and in fact other β-agonists in our environment.

References

Aboul-Enein, H.Y. and Serignese, V. (1999), "Quantitative determination of clenbuterol enantiomers in human plasma by high-performance liquid chromatography using the macrocyclic antibiotic chiral stationary phase teicoplanin1", *Biomed. Chromatogr.*, **13**(8), 520-524. https://doi.org/10.1002/(SICI)1099-0801(199912)13:8<520::AID-BMC919>3.0.CO;2-7

Almáši, M., Vargová, Z., Gyepes, R., Varga, R. and Zeleňák, V. (2014), "An unprecedented coordination mode of isonicotinate ligand in novel copper(II) polymeric complex: Synthesis, spectral, thermal and magnetic properties and their comparison with known molecular analog", *Inorg. Chem. Commun.*, **46**, 118-121. https://doi.org/10.1016/j.inoche.2014.05.026

Alves, T.C., Cabrera-Codony, A., Barceló, D., Rodriguez-Mozaz, S., Pinheiro, A. and Gonzalez-Olmos, R. (2018), "Influencing factors on the removal of pharmaceuticals from water with micro-grain activated carbon", *Water Res.*, **144**, 402-412. https://doi.org/10.1016/j.watres.2018.07.037

Armaya'u, U., Ariffin, M.M., Loh, S.H., Mohd Khalik, W.M.A.W. and Yusoff, H.M. (2022), "β-Agonist in the environmental waters: a review on threats and determination methods", *Green Chem. Lett. Rev.*, **15**(1), 232-251. https://doi.org/10.1080/17518253.2022.2032843

Aryee, A.A., Dovi, E., Guo, Q., Liu, M., Han, R., Li, Z. and Qu, L. (2021), "Selective removal of anionic dyes in single and binary system using Zirconium and iminodiacetic acid modified magnetic peanut husk", *Environ. Sci. Pollut. Res.*, **100**. https://doi.org/10.1007/s11356-021-13030-5

Benhafsa, F.M., Bouchama, A., Chadli, A., Tadjer, B. and Addad, D. (2022), "Comparative study of Pb (II) adsorption from water on used cardboard and powdered activated carbon", *Membr. Water Treat.*, **13**(2), 73-83. https://doi.org/10.12989/mwt.2022.13.2.073

Daughton, C.G. and Ternes, T.A. (1999), "Pharmaceuticals and personal care products in the environment: Agents of subtle change?", *Environ. Health Perspect.*, **107**(6), 907-938. https://doi.org/10.1289/ehp.99107s6907

David, N. and Dixon, E. (2015), "Synthesis, morphology and lead ion adsorption properties of metal organic frameworks of copper and cobalt", *Chem. Sci. J.*, **6**(4). https://doi.org/10.4172/2150-3494.1000113

de Ridder, D.J., Verliefde, A.R.D., Heijman, S.G.J., Verberk, J.Q.J.C., Rietveld, L.C., van der Aa, L.T.J., Amy, G.L. and van Dijk, J.C. (2011), "Influence of natural organic matter on equilibrium adsorption of neutral and charged pharmaceuticals onto activated carbon", *Water Sci. Technol.*, **63**(3), 416-423. https://doi.org/10.2166/wst.2011.237

Dhaka, S., Kumar, R., Deep, A., Kurade, M.B., Ji, S.W. and Jeon, B.H. (2019), "Metal-organic frameworks (MOFs) for the removal of emerging contaminants from aquatic environments", *Coord. Chem. Rev.*, **380**, 330-352. https://doi.org/10.1016/j.ccr.2018.10.003

Dotto, G.L., Costa, J.A.V. and Pinto, L.A.A. (2013),"Kinetic studies on the biosorption of phenol by nanoparticles from Spirulina sp. LEB 18", *J. Environ. Chem. Eng.*, **1**(4), 1137-1143. https://doi.org/10.1016/j.jece.2013.08.029

Hasan, Z. and Jhung, S. H. (2015), "Removal of hazardous organics from water using metal-organic frameworks (MOFs): Plausible mechanisms for selective adsorptions", *J. Hazard. Mater.*, **283**, 329-339. https://doi.org/10.1016/j.jhazmat.2014.09.046

Hemmati, M., Rajabi, M. and Asghari, A. (2017), "Ultrasound-promoted dispersive micro solid-phase extraction of trace anti-hypertensive drugs from biological matrices using a sonochemically synthesized conductive polymer nanocomposite", *Ultrason. Sonochem.*, **39**, 12-24. https://doi.org/10.1016/j.ultsonch.2017.03.024

Hignite, C. and Azarnoff, D. L. (1977), "Drugs and drug metabolites as environmental contaminants: Chlorophenoxyisobutyrate and salicylic acid in sewage water effluent", *Life Sci.*, **20**(2), 337-341. https://doi.org/10.1016/0024-3205(77)90329-0

Hong, S.H., Lee, C.G., Jeong, S. and Park, S.J. (2019), "Synthesis of polysulfone beads impregnated with Ca-sepiolite for phosphate removal", *Membr. Water Treat.*, **11**(1), 69-77. https://doi.org/10.12989/mwt.2020.11.1.069

Hu, M.L., Masoomi, M.Y. and Morsali, A. (2019), "Template strategies with MOFs", *Coord. Chem. Rev.*, **387**, 415-435. https://doi.org/10.1016/j.ccr.2019.02.021

Isiyaka, H.A., Jumbri, K., Sambudi, N.S., Zango, Z.U., Fathihah

Abdullah, N.A., Saad, B. and Mustapha, A. (2020), "Adsorption of dicamba and MCPA onto MIL-53(Al) metal-organic framework: Response surface methodology and artificial neural network model studies", *RSC Adv.*, **10**(70), 43213-43224. https://doi.org/10.1039/D0RA07969C

Kuppler, R.J., Timmons, D.J., Fang, Q.R., Li, J.R., Makal, T.A., Young, M.D., Yuan, D., Zhao, D., Zhuang, W. and Zhou, H.C. (2009), "Potential applications of metal-organic frameworks", *Coord. Chem. Rev.*, **253**(23-24), 3042-3066. https://doi.org/10.1016/j.ccr.2009.05.019

Kyzas, G.Z., Koltsakidou, A., Nanaki, S.G., Bikiaris, D.N. and Lambropoulou, D.A. (2015), "Removal of beta-blockers from aqueous media by adsorption onto graphene oxide", *Sci. Total Environ.*, **537**, 411-420. https://doi.org/10.1016/j.scitotenv.2015.07.144

Lan, Y., Coetsier, C., Causserand, C. and Groenen Serrano, K. (2018), "An experimental and modelling study of the electro-chemical oxidation of pharmaceuticals using a boron-doped diamond anode", *Chem. Eng. J.*, **333**(2017), 486-494. https://doi.org/10.1016/j.cej.2017.09.164

Li, C., Wu, Y.L., Yang, T., Zhang, Y. and Huang-Fu, W.G. (2010), "Simultaneous determination of clenbuterol, salbutamol and ractopamine in milk by reversed-phase liquid chromatography tandem mass spectrometry with isotope dilution", *J. Chromatogr. A*, **1217**(50), 7873-7877. https://doi.org/10.1016/j.chroma.2010.10.055

Li, P., Cheng, F.F., Xiong, W.W. and Zhang, Q. (2018), "New synthetic strategies to prepare metal-organic frameworks", *Inorg. Chem. Front.*, **5**(11), 2693-2708. https://doi.org/10.1039/c8qi00543e

Liu, Y.H., Lu, Y.L., Tsai, H.L., Wang, J.C. and Lu, K.L. (2001), "Hydrothermal synthesis, crystal structure, and magnetic property of copper(II) coordination networks with chessboard tunnels", *J. Solid State Chem.*, **158**(2), 315-319. https://doi.org/10.1006/jssc.2001.9118

Liu, Z., Zhang, B., Sun, J., Yi, Y., Li, M., Du, D., Zhu, F. and Luan, J. (2018), "Highly efficient detection of salbutamol in environmental water samples by an enzyme immunoassay", *Sci. Total Environ.*, 861-865. https://doi.org/10.1016/j.scitotenv.2017.08.324

Lu, J.Y. and Babb, A.M. (2002), "An extremely stable open-framework metal-organic polymer with expandable structure and selective adsorption capability", *Chem. Commun.*, **2**(13), 1340-1341. https://doi.org/10.1039/b200213b

Lv, J., Chen, Q., Liu, J.H., Yang, H.S., Wang, P., Yu, J., Xie, Y., Wu, Y.F. and Li, J.R. (2021), "Effective removal of clenbuterol and ractopamine from water with a stable Al(III)-based metal-organic framework", *Inorg. Chem.*, **60**(3), 1814-1822. https://doi.org/10.1021/acs.inorgchem.0c03296

Manousi, N. and Zachariadis, G.A. (2020), "Recent advances in the extraction of polycyclic aromatic hydrocarbons from environmental samples", *Molecules*, **25**(9), 2182. https://doi.org/10.3390/molecules25092182

Mansano Willig, J.C., Granetto, G., Reginato, D., Dutra, F.R., Poruczinski, É.F., de Oliveira, I.M., Stefani, H.A., de Campos, S.D., de Campos, É.A., Manarin, F. and Botteselle, G.V. (2020), "A comparative study between Cu(INA) 2 -MOF and [Cu(INA) 2 (H 2 O) 4] complex for a click reaction and the Biginelli reaction under solvent-free conditions", *RSC Adv.*, **10**(6), 3407-3415. https://doi.org/10.1039/C9RA10171C

Nakamoto, K. (2006), "Infrared and Raman Spectra of Inorganic and Coordination Compounds", *Handbook of Vibrational Spectroscopy*, 1872-1892. https://doi.org/10.1002/9780470027325.s4104

Nguyen, T.V., Ong, T.D., Lam, A.H.M., Pham, V.T., Phan, N.T. S. and Truong, T. (2017), "Nucleophilic trifluormethylation of aryl boronic acid under heterogeneous Cu(INA)2 catalysis at

room temperature: The catalytic copper-based protocol", *Mol. Catal.*, **436**, 60-66. https://doi.org/10.1016/j.mcat.2017.04.010

Perrotti, T.C., Freitas, N.S., Alzamora, M., Sánchez, D.R. and Carvalho, N.M.F. (2019), "Green iron nanoparticles supported on amino-functionalized silica for removal of the dye methyl orange", *J. Environ. Chem. Eng.*, **7**(4), 103237. https://doi.org/10.1016/j.jece.2019.103237

Petrović, M., Škrbić, B., Živančev, J., Ferrando-Climent, L. and Barcelo, D. (2014), "Determination of 81 pharmaceutical drugs by high performance liquid chromatography coupled to mass spectrometry with hybrid triple quadrupole-linear ion trap in different types of water in Serbia", *Sci. Total Environ.*, 415-428. https://doi.org/10.1016/j.scitotenv.2013.08.079

Pichon, A., Lazuen-Garay, A. and James, S.L. (2006), "Solvent-free synthesis of a microporous metal-organic framework", *CrystEngComm*, **8**(3), 211-214. https://doi.org/10.1039/b513750k

Policicchio, A., Filosa, R., Abate, S., Desiderio, G. and Colavita, E. (2017), "Activated carbon and metal organic framework as adsorbent for low-pressure methane storage applications: An overview", *J. Porous Mater.*, **24**(4), 905-922. https://doi.org/10.1007/s10934-016-0330-9

Quintana, J.B., Rodil, R. and Cela, R. (2012), "Reaction of β-blockers and β-agonist pharmaceuticals with aqueous chlorine: Investigation of kinetics and by-products by liquid chromatography quadrupole time-of-flight mass spectrometry", *Anal. Bioanal. Chem.*, **403**(8), 2385-2395. https://doi.org/10.1007/s00216-011-5707-7

Rodil, R., Quintana, J.B., Concha-Graña, E., López-Mahía, P., Muniategui-Lorenzo, S. and Prada-Rodríguez, D. (2012), "Emerging pollutants in sewage, surface and drinking water in Galicia (NW Spain)", *Chemosphere*, **86**(10), 1040-1049. https://doi.org/10.1016/j.chemosphere.2011.11.053

Sakai, N., Mohd Yusof, R., Sapar, M., Yoneda, M. and Ali Mohd, M. (2016), "Spatial analysis and source profiling of beta-agonists and sulfonamides in Langat River basin, Malaysia", *Sci. Total Environ.*, 43-50. https://doi.org/10.1016/j.scitotenv.2016.01.040

Sakai, N., Sakai, M., Mohamad Haron, D.E., Yoneda, M. and Ali Mohd, M. (2016), "Beta-agonist residues in cattle, chicken and swine livers at the wet market and the environmental impacts of wastewater from livestock farms in Selangor State, Malaysia", *Chemosphere*, **165**, 183-190. https://doi.org/10.1016/j.chemosphere.2016.09.022

Salem, A.A., Wasfi, I.A. and Al-Nassibi, S.S. (2012), "Trace determination of β-blockers and β2-agonists in distilled and waste-waters using liquid chromatography-tandem mass spectrometry and solid-phase extraction", *J. Chromatogr. B*, **908**, 27-38. https://doi.org/10.1016/j.jchromb.2012.09.026

Saruchi, and Kumar, V. (2019), "Adsorption kinetics and isotherms for the removal of rhodamine B dye and Pb +2 ions from aqueous solutions by a hybrid ion-exchanger", *Arab. J. Chem.*, **12**(3), 316-329. https://doi.org/10.1016/j.arabjc.2016.11.009

Schneemann, A., Bon, V., Schwedler, I., Senkovska, I., Kaskel, S. and Fischer, R.A. (2014), "Flexible metal-organic frameworks", *Chem. Soc. Rev.*, **43**(16), 6062-6096. https://doi.org/10.1039/c4cs00101j

Selkälä, T., Suopajärvi, T., Sirviö, J.A., Luukkonen, T., Lorite, G.S., Kalliola, S., Sillanpää, M. and Liimatainen, H. (2018), "Rapid uptake of pharmaceutical salbutamol from aqueous solutions with anionic cellulose nanofibrils: The importance of pH and colloidal stability in the interaction with ionizable pollutants", *Chem. Eng. J.*, **350**, 378-385. https://doi.org/10.1016/j.cej.2018.05.163

Slotkin, T.A. and Seidler, F.J. (2013), "Terbutaline impairs the development of peripheral noradrenergic projections: Potential implications for autism spectrum disorders and pharmacotherapy of preterm labor", *Neurotoxicol. Teratol.*, **36**, 91-96. https://doi.org/10.1016/j.ntt.2012.07.003

Soc, C., James, S.L., Adams, C.J., Bolm, C., Braga, D., Collier, P., Jones, W., Krebs, A., Mack, J., Maini, L., Orpen, A.G., Parkin, I.P., Shearouse, W.C., Steed, W., Waddell, D.C., James, S., Bolm, C., Braga, D., Collier, P., … Steed, J. (2012), "Mechanochemistry : Opportunities for new and cleaner synthesis", *Chem. Soc. Rev.*, **41**(1), 413-447. https://doi.org/10.1039/c1cs15171a

Song, J.Y. and Jhung, S.H. (2017), "Adsorption of pharmaceuticals and personal care products over metal-organic frameworks functionalized with hydroxyl groups: Quantitative analyses of H-bonding in adsorption", *Chem. Eng. J.*, **322**, 366-374. https://doi.org/10.1016/j.cej.2017.04.036

Spisso, B.F., Lopes, C.C., Marques, M.A.S. and Neto, F.R.A. (2000), "Determination of beta-agonists in bovine urine : Comparison of two extraction / clean-up procedures for high-resolution gas chromatography- mass spectrometry analysis", *J. Anal. Toxicol.*, **24**.

Stock, N. and Biswas, S. (2012), "Synthesis of metal-organic frameworks (MOFs): Routes to various MOF topologies, morphologies, and composites", *Chem. Rev.*, **112**(2), 933-969. https://doi.org/10.1021/cr200304e

Tang, Y., Gao, Z., Wang, S., Gao, X., Gao, J., Ma, Y., Liu, X. and Li, J. (2015), "Upconversion particles coated with molecularly imprinted polymers as fluorescence probe for detection of clenbuterol", *Biosens. Bioelectron.*, **71**, 44-50. https://doi.org/10.1016/j.bios.2015.04.005

Tang, Y., Lan, J., Gao, X., Liu, X., Zhang, D., Wei, L., Gao, Z. and Li, J. (2016), "Determination of clenbuterol in pork and potable water samples by molecularly imprinted polymer through the use of covalent imprinting method", *Food Chem.*, **190**, 952-959. https://doi.org/10.1016/j.foodchem.2015.06.067

Tella, A.C., Owalude, S.O., Ojekanmi, C.A. and Oluwafemi, O.S. (2014), "Synthesis of copper-isonicotinate metal-organic frameworks simply by mixing solid reactants and investigation of their adsorptive properties for the removal of the fluorescein dye", *New J. Chem.*, **38**(9), 4494-4500. https://doi.org/10.1039/c4nj00411f

Tella, A., Nwosu, F. and Adimula, V. (2016), "Removal of Anthracene from solution using [Cu(INA)2] metal- organic frameworks synthesized by a solvent free method", *Nigerian J. Mater. Sci. Eng.*, **7**, 26.

Ternes, T.A. (1998), "Occurrence of drugs in German sewage treatment plants and rivers", *Water Res.*, **32**(11), 3245-3260. https://doi.org/10.1016/S0043-1354(98)00099-2

Ternes, T. and Joss, A. (2015), "Human pharmaceuticals, hormones and fragrances - The challenge of micropollutants in urban water management", *Water Intell. Online*, **5**, 479. https://doi.org/10.2166/9781780402468

Toma, M., Sánchez, A., Casas, J., Sordo, J., García-Tasende, M., Castellano, E., Ellena, J. and Berdan, I. (2006), "New thallium(III) chloride complexes with pyridine carboxylic acids: From molecular compounds to supramolecular associations", *Open Chem.*, **1**(4), 441-464. https://doi.org/10.2478/bf02475227

Truong, T., Nguyen, C.V., Truong, N.T. and Phan, N.T.S. (2015), "Ligand-free N-arylation of heterocycles using metal-organic framework [Cu(INA) 2] as an efficient heterogeneous catalyst", *RSC Adv.*, **5**(130), 107547-107556. https://doi.org/10.1039/c5ra24165k

Valcárcel, Y., González Alonso, S., Rodríguez-Gil, J.L., Gil, A. and Catalá, M. (2011), "Detection of pharmaceutically active compounds in the rivers and tap water of the Madrid Region (Spain) and potential ecotoxicological risk", *Chemosphere*, **84**(10), 1336-1348. https://doi.org/10.1016/j.chemosphere.2011.05.014

Xing, G., Li, D., Woo, A.Y., Zhi, Z., Ji, L., Xing, R., Lv, H., He, B., An, H., Zhao, H., Lin, B., Pan, L. and Cheng, M. (2021), "Discovery of a highly selective β 2 - adrenoceptor agonist with a 2 - Amino-2-phenylethanol scaffold as an oral antiasthmatic agent", *J. Med. Chem.*, **65**(7), 5514-5527. https://doi.org/10.1021/acs.jmedchem.1c02006

Yan, K., Zhang, H., Hui, W., Zhu, H., Li, X., Zhong, F., Tong, X. and Chen, C. (2016), "Rapid screening of toxic salbutamol, ractopamine, and clenbuterol in pork sample by high-performance liquid chromatography—UV method", *J. Food Drug Anal.*, **24**(2), 277-283. https://doi.org/10.1016/j.jfda.2015.12.002

Yan, S., Yao, B., Lian, L., Lu, X., Snyder, S.A., Li, R. and Song, W. (2017), "Development of fluorescence surrogates to predict the photochemical transformation of pharmaceuticals in wastewater effluents", *Environ. Sci. Technol.*, **51**(5), 2738-2747. https://doi.org/10.1021/acs.est.6b05251

Yang, H., Wang, B., Cheng, J., Wang, R., Zhang, S., Dong, S., Wei, S., Wang, P. and Li, J.R. (2019), "Determination and removal of clenbuterol with a stable fluorescent zirconium (IV)-based metal organic framework", *Microchim. Acta*, **186**(7), 454. https://doi.org/10.1007/s00604-019-3586-3

Yu, Y. and Wu, L. (2011), "Comparison of four extraction methods for the analysis of pharmaceuticals in wastewater", *J. Chromatogr. A*, **1218**(18), 2483-2489. https://doi.org/10.1016/j.chroma.2011.02.050

Zango, Z.U., Abu Bakar, N.H.H., Sambudi, N.S., Jumbri, K., Abdullah, N.A.F., Kadir, E.A. and Saad, B. (2020), "Adsorption of chrysene in aqueous solution onto MIL-88(Fe) and NH2-MIL-88(Fe) metal-organic frameworks: Kinetics, isotherms, thermodynamics and docking simulation studies", *J. Environ. Chem. Eng.*, **8**(2), 103544. https://doi.org/10.1016/j.jece.2019.103544

Zango, Z.U., Jumbri, K., Sambudi, N.S., Ramli, A., Abu Bakar, N.H.H., Saad, B., Rozaini, M.N.H., Isiyaka, H.A., Jagaba, A.H., Aldaghri, O. and Sulieman, A. (2020), "A critical review on metal-organic frameworks and their composites as advanced materials for adsorption and photocatalytic degradation of emerging organic pollutants from wastewater", *Polymers*, **12**(11), 2648. https://doi.org/10.3390/polym12112648

Zhang, W., Wang, P. and Su, X. (2016), "Current advancement in analysis of β-agonists", *TrAC Trends Anal. Chem.*, **85**, 1-16. https://doi.org/10.1016/j.trac.2016.08.011

Zhou, Y.Y., Zhang, C.Y., Yan, Z.G., Li, K.J., Wang, L., Xie, Y.B., Li, F.S., Liu, Z. and Yang, J. (2012), "The use of copper(II) isonicotinate-based micro-solid-phase extraction for the analysis of polybrominated diphenyl ethers in soils", *Anal. Chim. Acta*, **747**(8), 36-41. https://doi.org/10.1016/j.aca.2012.08.023

CC